DOI: 10.1002/anie.201003364

Electronic Materials

Towards Tunable Graphene/Phthalocyanine–PPV Hybrid Systems**

*Jenny Malig, Norbert Jux, Daniel Kiessling, Juan-José Cid, Purificación Vázquez, Tomás Torres, and Dirk M. Guldi**

The sheer explosion of interest in graphene has undoubtedly shown that it is the rising star in the emerging field of nanotechnology.[1] Its extraordinary properties render it an outstanding material for electronics, material sciences, and photoconversion systems. As a zero-gap semiconductor for example, a flat monolayer of graphene is almost transparent and exhibits the lowest known electrical resistivity for any material at room temperature.[2] The remarkably high electron mobility of graphene gives rise to its implementation in transparent conducting electrodes as a viable alternative to indium tin oxide (ITO).[3,4] Recent results demonstrate, however, that doping is a necessity to harvest the full potential of graphene.[5,6] Therefore, the aim herein is the tuning/altering of the features of photochemically transparent graphene by integrating a versatile electron donor system in solution.

High-quality graphene flakes have been formed by means of solution processing, which involves exfoliating and dispersing them directly from graphite.[7,8] Such mild strategies stand in strong contrast to high throughput exfoliation of graphite with the assistance of strong oxidants.[9–11] Moreover, reduction of graphene oxide to graphene is by no means quantitative and results in irreversible coagulation and permanent lattice defects.[12,13] To date, samples that exhibit high charge mobilities[14] are large-area graphene samples obtained by micromechanical cleavage of pyrrolitic graphite.[15] Other notable breakthroughs in this area rely on sheets grown onto solid substrates.[16–19]

The investigation of novel electron donor–acceptor hybrids involving low-dimensional allotropes of carbon is far more challenging than the exploitation of carbon nanotubes in the same context. The reason is primarily the lack of photospectroscopic signatures/markers, which makes the study of graphene more challenging. In fact, we have selected a spectator molecule to circumvent this impediment and to assist in identifying and visualizing electron donor–acceptor interactions. The unique absorption with high extinction coefficients in the red and near infrared regions, fluorescence, and the strong electron-donating character of zinc phthalocyanines (ZnPc) make a ZnPc-based PPV oligomer (**1**)[19] PPV = poly(*p*-phenylene vinylene) the molecule of choice (Supporting Information, Scheme S1). Apart from supporting several ZnPc units, the oligomeric backbone is expected to be a great asset with regard to graphite exfoliation and stabilization of novel nanographene (NG) hybrids bearing ZnPc oligomer **1** that are thus formed (Figure 1).

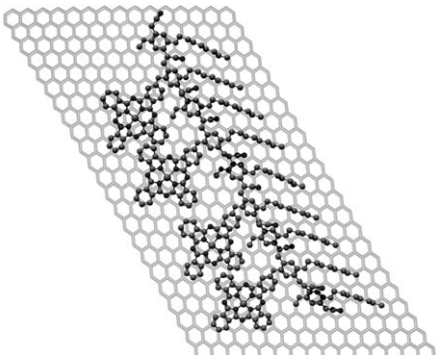

Figure 1. View of an exfoliated NG/**1** hybrid.

In the absorption spectrum of ZnPc oligomer **1**, the typical signature of ZnPc, that is, maxima at around 346 nm (that is, the Soret band) and 610/675 nm (the Q band) is observed. Furthermore, the π–π* transitions of the PPV are discernible as a weak shoulder at about 440 nm. In the corresponding emission spectrum, only the prominent features of the red-emitting ZnPc evolve owing to an intramolecular energy-transfer reaction.[20]

In the next step, pure natural graphite was suspended and exfoliated in THF solutions of ZnPc oligomer **1** (10^{-6} M). Upon ultrasonication and centrifugation, the supernatant was subjected to spectroscopic, microscopic, and thermogravimetric investigations (Supporting Information, Figure S2). For the thermogravimetric investigations, the supernatant was filtered and washed with THF several times. After drying the

[*] Dr. J.-J. Cid, Prof. P. Vázquez, Prof. T. Torres
Departamento de Química Orgánica & IMDEA-Nanociencia
Universidad Autónoma de Madrid, Cantoblanco
28049 Madrid (Spain)
J. Malig, Priv.-Doz. Dr. N. Jux, D. Kiessling, Prof. D. M. Guldi
Department of Chemistry and Pharmacy and
Interdisciplinary Center for Molecular Materials (ICMM)
Friedrich-Alexander-Universität Erlangen-Nürnberg
91058 Erlangen (Germany)
E-mail: guldi@chemie.uni-erlangen.de
Homepage: http://www.chemie.uni-erlangen.de/dcp/assets/pdf/DCP-Profile2010.pdf

[**] Financial support from the DFG (Cluster of Excellence – Engineering of Advanced Materials), GSMS, ICMM, ZMP, MICINN, and MEC (Spain) (CTQ2008-00418/BQU, PLE2009-0070, PSE-120000-2009-008 FOTOMOL, and Consolider-Ingenio Nanociencia Molecular CSD2007-00010), Comunidad de Madrid (MADRISOLAR-2, S2009/PPQ/1533) and EU (MRTN-CT-2006-035533 Solar-N-type and Project ROBUST DSC FP7-Energy-2007-1-RTD, N° 212792) is gratefully acknowledged. PPV = poly(*p*-phenylene vinylene).

Supporting information for this article is available on the WWW under http://dx.doi.org/10.1002/anie.201003364.

filter cake in vacuum, the analysis was carried out. A significant weight loss of 6.3% was obtained between 100–300 °C, which is characteristic of physisorbed functional groups; by estimating and comparing the area of the ZnPc oligomer with that of graphene, a total coverage of 35% can be assumed.

Regarding the absorption characteristics of **1**, a significant broadening and decrease in intensity dominates the spectrum in the presence of graphene. In Figure 2, the latter is

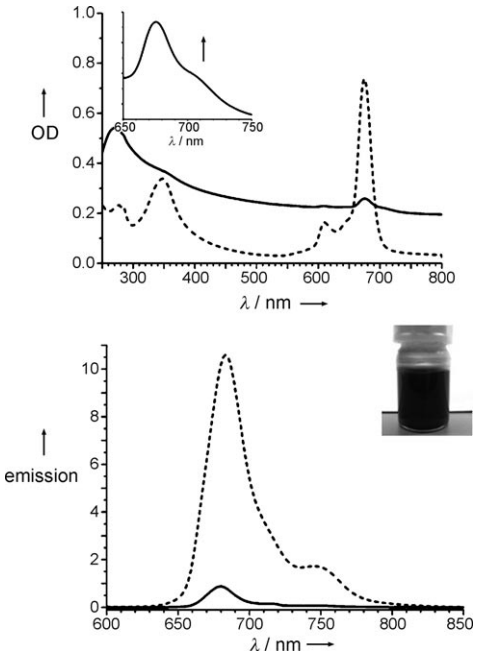

Figure 2. Upper: absorption spectra of **1** (-----) and NG/**1** (——) in THF; the inset shows the 650 to 750 nm range in more detail. Lower: emission spectra of **1** (-----) and NG/**1** (——) in THF with suspensions that exhibit the same optical absorbance at the 350 nm excitation wavelength.

discernable in the form of absorption features that include a maximum centered at 270 nm. A closer look reveals that the long wavelength transition at 675 nm transforms into a new fingerprint that exhibits a maximum at 707 nm. A 32 nm bathochromic shift reflects the strong electronic coupling between the individual components in what is presumed to be NG/**1** hybrid. Notably, addition of variable Triton X-100 concentrations (Supporting Information, Figure S2) replaces **1** in NG/**1** from the graphene surface and, in turn, the original absorption of **1** in the entire 250 to 800 nm range is restored.

Figure 2 illustrates that upon 350 nm excitation, which corresponds to the Soret-band absorption of ZnPc, the ZnPc fluorescence of the NG/**1** hybrid is quenched nearly quantitatively. Upon correcting for the different absorption cross-sections, that is, graphene versus ZnPc, the quenching is quantified as being more than 60%. Comparing the relative quantum yields by a modified gradient method assists in ruling out inner filter effects (Supporting Information, Figure S3). A value of 3.1 ns was registered for **1** in the absence of graphene (Supporting Information, Figure S4) by fluorescence lifetime measurements. In the presence of graphene, that is, the exfoliated NG/**1** hybrids, the same value was registered, but with much lower intensity ($\ll$65%). To this end, the latter reflects free ZnPc oligomer (**1**) that is present in suspension. The intrinsic decay in the NG/**1** hybrid, on the other hand, is restricted by the instrumental response of our single-photon counting apparatus. Insights into the dynamics, that is, electron transfer versus energy transfer, were, however, derived from other time-resolved measurements.

That graphite is exfoliated into up to micrometer-sized graphene flakes was supported by microscopical analysis. First, the NG/**1** suspension was spin-coated onto a silicon oxide substrate (a 300 nm thick oxide layer) to accomplish optical microscopy (Supporting Information, Figure S5).[21] The starting material, that is, high crystalline graphite flakes, were then uniformly disintegrated into mono-/few-layer graphene with regular flake size. Atomic force microscopy (AFM) analysis revealed large areas of homogenously exfoliated graphite (Supporting Information, Figure S6). Single flake analysis confirmed that monolayer graphene tends to either roll up or fold up to yield intertwined sheets, while equilibriating in solution or during the deposition process, which was corroborated by transmission electron microscopy (TEM; Figure 3). Importantly, the resulting

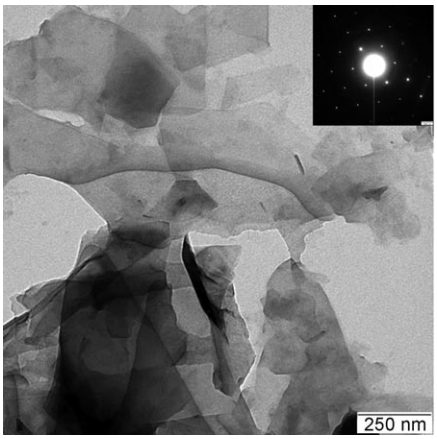

Figure 3. TEM image and selected area electron diffractogram (inset) of NG/**1** drop-casted onto a carbon-coated copper grid.

sheets consist in general of individual mono- and/or few-layer graphene flakes randomly stacked onto each other, as emphasized by the selected-area electron diffractogram.

Further insights came from nonresonant and resonant Raman experiments of the NG/**1** spin-coated onto silicon oxide substrates with 532 and 633 nm excitation, respectively. In nonresonant experiments (Supporting Information, Figure S7), the typical Raman signals for exfoliated graphite, namely the D band at 1351 cm^{-1}, the G band at 1584 cm^{-1}, and the 2D band around 2720 cm^{-1} emerge. Upon exfoliation, the G band blue-shifts by about 3–5 cm^{-1} relative to the bulk graphite material (1582 cm^{-1}).[22] Another notable difference is that the 2D band, which is highly asymmetric in the crystalline starting material, converts into a highly symmetric shape upon exfoliation. This change in symmetry, which is a

result of successfully exfoliated graphite, is further accompanied by a red-shift; that is, from 2724 to 2696 cm^{-1}.

TEM studies confirmed that reaggregation governs the overall thermodynamic stability of exfoliated NG/**1**, and the disintegration of graphite-like AB stacks is undoubtedly confirmed by our Raman investigations. In fact, a more turbostratic bulk structure evolves. Finally, an increase in D and D′ band intensity, that is 1350 cm^{-1} and 1621 cm^{-1}, respectively, parallels the exfoliation and is attributed to smaller flake sizes and, in turn, a larger edge contribution, which provides the necessary crystal defects to activate the underlying double resonant Raman processes.[23,24]

In resonant experiments (Figure 4, upper part), in which the excitation wavelength is tuned to match the optical transition energy of ZnPc in **1**, Raman peaks of the latter

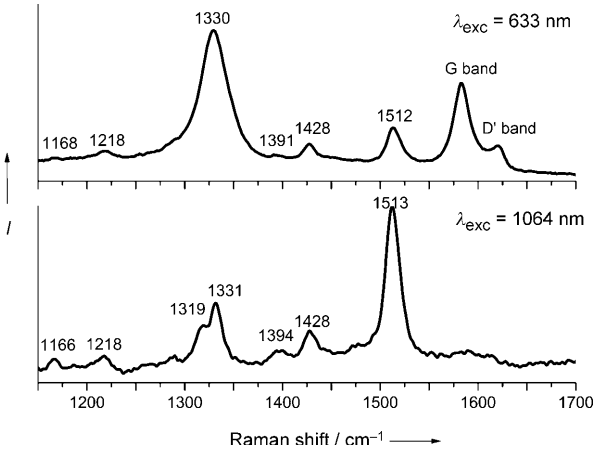

Figure 4. Upper: Raman spectrum of **1** with 633 nm excitation. Lower: Raman spectrum of NG/**1** with 1064 nm excitation. The labeled peaks are assigned to ZnPc vibrations.

should be detectable. As fluorescence cross-sections are, however, much larger than Raman cross-sections, fluorescing features typically dominate the spectral response and, in turn, characteristic Raman peaks of ZnPc are hardly ever seen. In fact, this is the case when the ZnPc oligomer **1** alone is measured.

Graphene exhibits density of states below and above the Fermi energy owing to the linear dispersion relation near the high symmetry K point of the first Brillouin zone. Therefore, graphene may act as either an electron donor or as an electron acceptor, resulting in fluorescence quenching by either electron transfer to or from ZnPc.[25] Evidence for such a process would attest the electronic communication in the NG/**1** hybrid. Recent advances in implementing graphene in fluorescence quenching microscopy[26] and resonance experiments with chromophores should be noted.[27,28]

In line with the aforementioned fluorescence experiments, which give rise to the coexistence of strongly quenched NG/**1** hybrids and strongly emitting free ZnPc oligomer **1**, 633 nm excitation of a spin-coated sample of NG/**1** onto silicon surfaces reveals two different types of materials (Supporting Information, Figure S8). On one hand, crystallites are discernable that strongly fluoresce; these undoubtedly relate to free ZnPc oligomer **1**. On the other hand, nonfluorescing flakes are seen, and new strong Raman peaks evolve (Supporting Information, Figure S8). A comparison with the nonresonant Raman spectrum of **1** at 1064 nm excitation wavelength is therefore decisive (Figure 4, lower part). In both cases, dominant Raman peaks are found at 1220, 1331, 1429, and 1513 cm^{-1}, the origin of which are pyrrolic vibrations. We assign the 1331 cm^{-1} band to C_α–C_β vibrations, while the 1513 cm^{-1} band is indicative for C_β–C_β symmetric stretching vibrations. Finally, the band at 1429 cm^{-1} is associated with C–N stretching vibrations, which reflects the polymorphic structure.[29]

After this more qualitative analysis of NG/**1** interactions, we turned to femtosecond transient absorption measurements following excitation at 387 and 700 nm. The incentive was to gather quantitative insights, both kinetically and spectroscopically, into the nature of the interactions. Notably, 387 nm is a rather unspecific excitation wavelength, as NG/**1** and free ZnPc oligomer **1** all absorb at this wavelength. 700 nm, on the other hand, addresses exclusively NG/**1** owing to the lack of appreciable ZnPc absorptions.

In reference experiments, that is, excitation of **1** (at 387 nm; Supporting Information, Figure S9), the following features evolve essentially with the conclusion of the excitation: minima at 610/670 nm and maxima at 485/630/820/1290 nm. These processes can be ascribed to singlet excited state features that transform during the subsequent 3 ns into the corresponding triplet excited state features. For the latter, a minimum at 680 nm and a maximum at 500 nm were seen to grow concomitantly with the decay of the former.[30]

For NG/**1**, minima evolve within the first picoseconds in the visible (615, 670, 705, and 740 nm) and in the near-infrared regions (1200 nm; Figure 5). In line with the absorption assays, we ascribe the features at 670 and 705 nm to free ZnPc oligomer **1** and NG/**1**, respectively. Reference experiments with NG (Supporting Information, Figure S10) verify that the minima at 615 and 1200 nm correlate with graphene-related transitions. A common feature of all of these features is that they are metastable and that they decay within 4 ps ($k_{CS} = 7.1 \times 11^{11}\ s^{-1}$). As a consequence of this intrinsically fast decay, new characteristics develop. Most prominent is the maximum in the visible at 840 nm, which corresponds to the one-electron oxidized form of ZnPc. Furthermore, a rather broad bleaching is observed in the near-infrared that reveals a local minimum at 1290 nm. When considering the underlying red-shift from 1200 to 1290 nm, a close resemblance with the reduction of semiconducting SWNT is observed.[31] In other words, an electron transfer occurs that evolves from the photoexcited ZnPc as electron donor to graphene as electron acceptor. From a multiwavelength analysis, we derive a lifetime of 360 ps ($k_{CR} = 2.7 \times 10^9\ s^{-1}$) for the correspondingly formed electron-transfer product. At time delays beyond 500 ps, the singlet excited-state features of the free ZnPc oligomer **1** remain visible, as they undergo slow intersystem crossing to the triplet manifold. In terms of energetics, we consider the ease of oxidizing **1**, namely, 0.6 V versus SCE, as an indicator for a strongly exothermic electron transfer of about 1.0 eV.

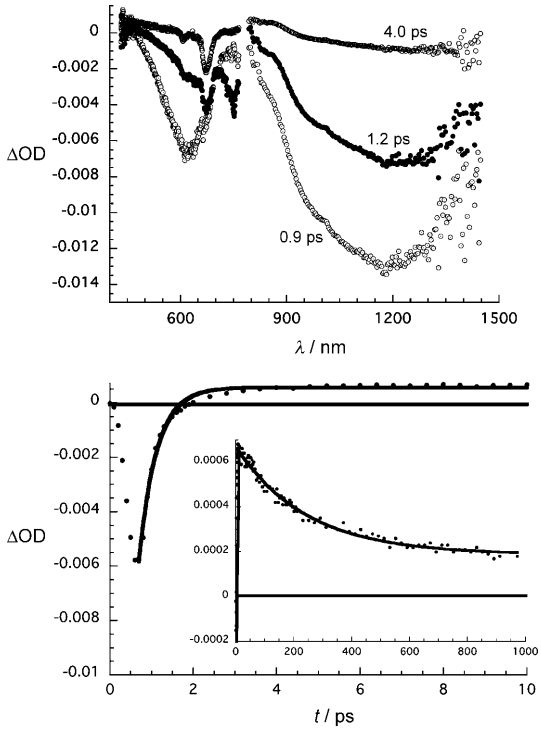

Figure 5. Upper: differential absorption spectra (visible and near-infrared) obtained by femtosecond flash photolysis (387 nm) of NG/**1** in THF with several time delays between 0 and 4 ps at room temperature. Lower: time–absorption profiles (0 to 10 ps) of the spectra shown above at 850 nm monitoring the forward electron transfer; inset shows the time–absorption profile (0 to 1000 ps) of the spectra shown above at 850 nm monitoring the backward electron transfer.

Finally, the exfoliated NG/**1** was excited into its fingerprint region at 700 nm (Supporting Information, Figure S11). Again, the electron transfer product characteristics, which are most notable at 840 and 1290 nm, evolve with kinetics that are somehow faster than in the 387 nm excitation, that is, 2 ps. The faster kinetics are understood on the basis that 387 nm excitation generates a locally excited state (ZnPc), which transforms somewhat slower into the radical ion-pair state compared to the 700 nm experiment. In fact, the latter correlates with excitation of the electronically coupled state. Importantly, there is a lack of any appreciable contributions from free ZnPc oligomer **1** in these experiments. In line with this assumption is the observation that at time delays exceeding 500 ps, no notable features remain discernable.

Encouraged by the aforementioned results, we explored the potential of of NG/**1** in solar energy conversion applications and have manufactured a prototype solar cell by means of transfer deposition of NG/**1** from a 0.2 μm pore-sized PTFE filter to ITO and quartz substrate, respectively. SEM investigations show that NG/**1** homogeneously covers the substrate surface and form a membrane-like film (Supporting Information, Figure S12). In initial experiments, four-point probe resistivity measurements were recorded, which test the conductive electrode properties and photocurrents under white-light illumination. NG/**1** acts as an active layer, and the tests emphasize the versatility of this new hybrid material. A conductive film for NG/**1** with a sheet resistivity of 90 kOhm/□ at 75% transmittance (550 nm) was observed (Supporting Information, Figure S13). Under short-circuit conditions, a photocathodic behavior was observed, which is indicative of electrons that flow from ITO to the film. The photoaction spectra of the different cells with I^-/I_3^- (0.5 M/0.01 M) electrolyte under monochromatic conditions were used to determine the incident photon-to-current conversion efficiency (IPCE). In line with what has been noted in the absorption spectra, broad and featureless transitions emerge in the photoaction spectrum between 350 and 720 nm. The maximum IPCE values, which reach 0.3%, are intriguing (Supporting Information, Figure S14). Despite the fact that the photoelectrochemical cells are not optimized, we have demonstrated a versatile approach to integrate a donor molecule upon graphene by concomitant exfoliation of graphite.

In short, we have obtained high-quality graphene flakes by processing THF solutions of a ZnPc oligomer (**1**). The species **1** interacts tightly and reversibly with graphene, affording uniquely stable dispersions with high concentrations of mono- to few-layer graphene. In fact, the PPV backbone is beneficial not only with respect to function as a template for several ZnPc but also to increase the overall π–π interactions with graphene.[29] In the exfoliated NG/**1** hybrids, strong electronic coupling between the individual components prevails and gives rise to new fingerprint absorptions and a nearly quantitatively quenching of ZnPc fluorescence. Transient absorption measurements confirm that the nature of these interactions is electron transfer from ZnPc to graphene, both in the ground and in the excited state, to afford a electron-transfer product that survives for several hundred picoseconds (Figure 6). Our approach thus yields novel

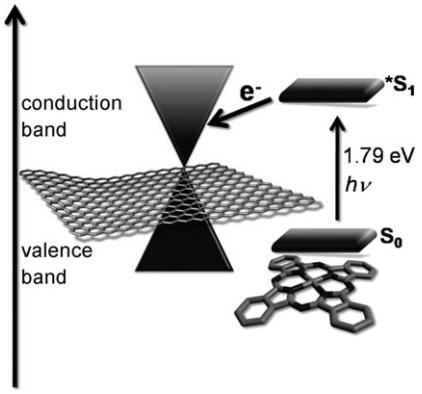

Figure 6. Electron-transfer pathway in the exfoliated NG/**1** hybrid.

hybrid materials, which were tested both as an active layer and transparent electrode material for solar-cell applications. Devices in which the electronic structure of graphene is tuned by chemical functionalization in an appropriate manner are thus conceivable where all of the assemblies consist entirely of graphene.

Received: June 3, 2010
Revised: October 31, 2010
Published online: March 9, 2011

Keywords: electron transfer · graphene · phthalocyanines · time-resolved spectroscopy

[1] A. K. Geim, K. S. Novoselov, *Nat. Mater.* **2007**, *6*, 183.
[2] M. S. Fuhrer, S. Adam, *Nature* **2009**, *458*, 38.
[3] X. Wang, L. Zhi, K. Müllen, *Nano Lett.* **2007**, *8*, 323.
[4] G. Eda, G. Fanchini, M. Chhowalla, *Nat. Nanotechnol.* **2008**, *3*, 270.
[5] S. De, J. N. Coleman, *ACS Nano* **2010**, *4*, 2713.
[6] B. Das, R. Voggu, C. S. Rout, C. N. R. Rao, *Chem. Commun.* **2008**, 5155.
[7] Y. Hernandez, V. Nicolosi, M. Lotya, F. M. Blighe, Z. Sun, S. De, I. T. McGovern, B. Holland, M. Byrne, Y. K. Gun′Ko, J. J. Boland, P. Niraj, G. Duesberg, S. Krishnamurthy, R. Goodhue, J. Hutchison, V. Scardaci, A. C. Ferrari, J. N. Coleman, *Nat. Nanotechnol.* **2008**, *3*, 563.
[8] J. M. Englert, J. Röhrl, C. D. Schmidt, R. Graupner, M. Hundhausen, F. Hauke, A. Hirsch, *Adv. Mater.* **2009**, *21*, 4265.
[9] W. S. Hummers, R. E. Offeman, *J. Am. Chem. Soc.* **1958**, *80*, 1339.
[10] B. Brodie, *Ann. Chim. Phys.* **1860**, *59*, 466.
[11] L. Staudenmaier, *Ber. Dtsch. Chem. Ges.* **1898**, *31*, 1481.
[12] I. Jung, D. Dikin, R. Piner, R. Ruoff, *Nano Lett.* **2008**, *8*, 4283.
[13] C. Gómez-Navarro, R. T. Weitz, A. M. Bittner, M. Scolari, A. Mews, M. Burghard, K. Kern, *Nano Lett.* **2007**, *7*, 3499.
[14] X. Du, I. Skachko, A. Barker, E. Andrei, *Nat. Nanotechnol.* **2008**, *3*, 491.
[15] K. Novoselov, D. Jiang, F. Schedin, T. Booth, V. Khotkevich, S. Morozov, A. Geim, *Proc. Natl. Acad. Sci. USA* **2005**, *102*, 10451.
[16] P. Sutter, J. Flege, E. Sutter, *Nat. Mater.* **2008**, *7*, 406.
[17] C. Berger, Z. Song, X. Li, X. Wu, N. Brown, C. Naud, D. Mayou, T. Li, J. Hass, A. Marchenkov, *Science* **2006**, *312*, 1191.
[18] A. Reina, X. Jia, J. Ho, D. Nezich, H. Son, V. Bulovic, M. Dresselhaus, J. Kong, *Nano Lett.* **2009**, *9*, 30.
[19] K. V. Emtsev, A. Bostwick, K. Horn, J. Jobst, G. L. Kellogg, L. Ley, J. L. McChesney, T. Ohta, S. A. Reshanov, J. Röhrl, E. Rotenberg, A. K. Schmid, D. Waldmann, H. B. Weber, T. Seyller, *Nat. Mater.* **2009**, *8*, 203.
[20] J. Cid, C. Ehli, C. Atienza-Castellanos, A. Gouloumis, E. Maya, P. Vázquez, T. Torres, D. Guldi, *Dalton Trans.* **2009**, 3955.
[21] C. Backes, J. Englert, N. Bernhard, F. Hauke, A. Hirsch, *Small* **2010**, *6*, 1968.
[22] A. Ferrari, J. Meyer, V. Scardaci, C. Casiraghi, M. Lazzeri, F. Mauri, S. Piscanec, D. Jiang, K. Novoselov, S. Roth, *Phys. Rev. Lett.* **2006**, *97*, 187401.
[23] B. Krauss, P. t. Nemes-Incze, V. Skakalova, L. s. P. Biro, K. von Klitzing, J. H. Smet, *Nano Lett.* **2010**, *10*, 4544.
[24] M. Pimenta, G. Dresselhaus, M. Dresselhaus, L. Cancado, A. Jorio, R. Saito, *Phys. Chem. Chem. Phys.* **2007**, *9*, 1276.
[25] A scenario arises that resembles interactions with a metal surface, where the quenching of the fluorescence is quenched owing to efficient resonant energy transfer.
[26] J. Kim, L. Cote, F. Kim, J. Huang, *J. Am. Chem. Soc.* **2010**, *132*, 260.
[27] N. V. Kozhemyakina, J. M. Englert, G. Yang, E. Spiecker, C. D. Schmidt, F. Hauke, A. Hirsch, *Adv. Mater.* **2010**, *22*, 5483.
[28] L. Xie, X. Ling, Y. Fang, J. Zhang, Z. Liu, *J. Am. Chem. Soc.* **2009**, *131*, 9890.
[29] C. Jennings, R. Aroca, A. Hor, R. Loutfy, *J. Raman Spectrosc.* **2005**, *15*, 34.
[30] 700 nm excitation of ZnPc oligomer fails to generate any significant transient features.
[31] M. Herranz, C. Ehli, S. Campidelli, M. Gutierrez, G. Hug, K. Ohkubo, S. Fukuzumi, M. Prato, N. Martin, D. Guldi, *J. Am. Chem. Soc.* **2008**, *130*, 66.

